Assessment of mixing quality in full-scale, biogas-mixed anaerobic digestion using CFD

Davide Dapelo[a,*], John Bridgeman[a]

[a]*Faculty of Engineering and Informatics, University of Bradford, Bradford BD7 1DP, United Kingdom*

Abstract

An Euler-Lagrange CFD model is applied to a full-scale, biogas-mixed anaerobic digester to improve mixing efficiency and improve overall performance.

Two quantitative mixing criteria previously adopted in anaerobic digestion (viz., uniformity index and dead volume) are critically assessed for the first time. A novel qualitative method is introduced to clarify the output of the quantitative methods. The first-ever quantitative assessment of mixing quality in full-scale, biogas-mixed anaerobic digestion is then proposed, and a strategy to improve mixing, involving the combined use of concentric nozzle manifolds at the base of the digester, is evaluated.

Keywords: Industrial-scale anaerobic digestion, CFD, Euler-Lagrange, Mixing Assessment, Optimisation of performance

*Corresponding author.
Address: B2.20, Chesham Building, Bradford BD7 1DP, United Kingdom
Email: ddapelo@bradford.ac.uk
Tel: +44 1274 23 3686

Nomenclature

α	Relative occupancy
χ	Non-diffusive numerical tracer
$\dot{\gamma}$	Shear rate, s^{-1}
Co	Courant number
μ	Power-law viscosity, $\mathrm{Pa\,s}$
τ	Shear stress, Pa
τ_0	Herschel-Bulkley critical shear stress, Pa
$\mathbf{u}$	Liquid phase velocity field, $\mathrm{m\,s}^{-1}$
Ξ	Rectangular function
I	Tracer concentration interval
K	Power-law consistency coefficient, Pa s^n
n	Power-law index
t	Time, s
V	Volume, m^3
CFD	Computational Fluid Dynamics
GCI	Grid Convergence Index
UI	Uniformity Index

1. Introduction

The wastewater industry is expected to face unprecedented pressures in the forthcoming decades. The worldwide demand for clean water is growing, with 50% more food and 30% more water needed by 2030 (WWAP (World Water Assessment Programme), 2012). In addition, tightening EU regulations (specifically, the Water Framework Directive, WFD) will cause wastewater treatment works (WwTWs) to increase energy consumption by up to 60% in the next 10-15 years (European Environment Agency, 2015). The need to mitigate and adapt to climate change imposes renewed efforts towards energy efficiency and energy reuse, and hence it is clear that the link between wastewater and energy must be addressed (Dapelo and Bridgeman, 2018).

In 2010-2011, WwTWs in the UK produced 1.5M tonnes of municipal sewage sludge, the by-product of wastewater treatment (WaterUK, 2012). Sludge is often treated using mesophilic anaerobic digestion in which it is mixed with anaerobic bacteria at temperatures between 22 and 41°C. As biodegradable material is broken down into more stable compounds, a methane-rich biogas is produced and subsequently harnessed as a renewable energy via combined heat and power technology. Although mixing is responsible for 17–73% of the energy consumption of an industrial digester (Owen, 1982), current practice in digester design is still rooted in rules of thumb and empiricism rather than science (Dapelo et al., 2015). Therefore, there is an urgent need to revise the way mixing is designed and operated within industrial digesters in order to improve the balance between input mixing energy and biogas output—i.e. to reduce input mixing power without compromising, and indeed enhancing, biogas yield. (Dapelo and Bridgeman, 2018). Recent experimental evidence (Kress et al., 2018) shows that it is possible to halve input mixing power without impacting nutrient distribution.

Computational fluid dynamics (CFD) is a powerful tool that can be used to study flow patterns of non-Newtonian sludge and mixing (Vesvikar and Al-Dahhan, 2005; Karim et al., 2007; Meroney and Colorado, 2009; Terashima et al., 2009; Wu, 2010; Bridgeman, 2012; Sindall et al., 2013; Craig et al., 2013; Dapelo et al., 2015; Hurtado et al., 2015; Zhang et al., 2016; Dapelo and Bridgeman, 2018; Lebranchu et al., 2017; Meister et al., 2018). However, the work undertaken so far is limited. First of all, whilst biogas mixing, both confined (i.e., biogas injection performed inside an internal draft tube) and unconfined (i.e., without internal draft tube), is commonplace (despite not being the most efficient way of mixing: Brade and Noone 1981; Wu 2010) as the lack of moving elements inside digesters reduces wear and maintenance, the amount of literature dedicated to it is still very limited when compared to other forms of mixing. Only Vesvikar and Al-Dahhan (2005); Wu (2010, 2012b, 2014); Dapelo et al. (2015); Dapelo and Bridgeman (2018) have proposed robust multiphase models and only Wu (2010, 2012b, 2014); Dapelo and Bridgeman (2018) have considered full-scale digesters.

Another limitation of CFD work undertaken to date is the lack of a clear criterion to assess mixing quality. Camp and Stein (1943) proposed the average shear rate as the fundamental process characteristic to classify mixing in vessels, and the water industry traditionally adopts the approach of considering digester mixing as satisfactory when the average shear rate exceeds 50—80 s^{-1} (Tchobanoglous et al., 2010). However, this criterion has been shown to be inadequate for the case of sludge mixing for anaerobic digestion. Previous laboratory-based and full-scale work has demonstrated that anaerobic digestion takes place under a much lower average shear rate—up to one order of magnitude lower for laboratory-scale (Bridgeman, 2012; Sindall et al., 2013), and two orders of magnitude lower for full-scale (Dapelo and Bridgeman, 2018).

Furthermore, the approach of minimum average shear rate has been criticized on the basis that the representation of complex flow patterns through one number is something of an over-simplification (Clark, 1985), especially considering that, in a mixed tank, areas of high local shear rate and dead zones are likely to coexist (Bridgeman, 2012; Sindall et al., 2013; Dapelo et al., 2015). However, there is no universally-accepted alternative approach in the literature.

Meroney and Colorado (2009); Terashima et al. (2009); Hurtado et al. (2015) evaluated the mixing performance of different full-scale digesters through CFD simulations of tracer washout parameters (viz. turnover time and dead volume) and tracer response curve. This approach avoids costly and time-consuming fieldwork experiments and has the fundamental advantage of providing an evaluation of mixing quality before digester construction.

However, it only gives a "black box" representation of the flow through the digester (Dapelo and Bridgeman, 2018). Meroney and Colorado (2009); Hurtado et al. (2015) evaluated velocity, turbulence intensity and tracer flow patterns and passive Lagrangian particle distributions, but their analyses were limited to qualitative considerations.

Hurtado et al. (2015) followed Vesvikar and Al-Dahhan (2005) and defined the dead volume as the portion of domain where velocity magnitude was below 5% of the maximum velocity. However, this method does not constitute a comprehensive evaluation of mixing because the choice of the minimum threshold of 5% is arbitrary, and local variations of velocity magnitude may unrealistically alter the definition of dead zone. (Dapelo and Bridgeman, 2018) followed the idea that higher shear rate values imply better mixing. However, instead of providing a simple average figure as in Tchobanoglous et al. (2010), local shear values were used to identify very low, low, average and high shear rate zones within the computational domain, and the volume ratio of such zones over the whole volume were compared to each other in order to assess mixing quality. This method was successful in ascertaining that the digester design considered was subject to over-mixing. However, the approach provided only comparative data, and failed to provide information when mixing was time-dependent (i.e., when biogas injection was switched between two different nozzle series).

To date, the only attempt to introduce a quantitative, unequivocal criterion for mixing quality that takes into account the complexity of the flow patterns within a closed tank is that of Terashima et al. (2009). A non-diffusive tracer was defined throughout the computational domain, and the uniformity index (UI) was defined as the tracer's absolute relative mean deviation. UI was used to assess different impeller mixing regimes and sludge total solid (TS) contents. However, Terashima et al. (2009) considered only draft-tube impeller mixing, and the analysis incorporated a number of limitations, including a limitation on time-independent mixing, and application only to laminar flow.

To address the lack of biogas-mixed anaerobic digestion CFD modelling, a two-phase Euler-Lagrangian model was developed and validated against lab-scale experimental data (Dapelo et al., 2015; Sindall et al., 2017). Dapelo and Bridgeman (2018), explained the difficulty of validating CFD models involving opaque sludge, and proposed a two-fold approach of a lab-scale validation of the model (which was performed in (Dapelo et al., 2015; Sindall et al., 2017), and applying the validated data to a set of full-scale scenarios. The inherent advantages of the Euler-Lagrangian formulation over other two-phase models have been explained elsewhere (Dapelo et al., 2015; Dapelo and Bridgeman, 2018). In addition to the above-mentioned evaluation of mixing through shear rate relative occupancy assessment, a full-scale application of the model (Dapelo and Bridgeman, 2018) showed for the first time the potential beneficial effect of time-dependent mixing—in particular, switching biogas injection between two different nozzle series at regular time intervals was shown to counter viscosity-driven short-circuiting, and greatly improved the spread of a numerical, non-diffusive scalar tracer. However, the mixing criterion based on shear rate relative occupancy evaluation failed to provide quantitative information.

Within the work described in this paper, a comprehensive set of different biogas-mixing methods for full-scale anaerobic digestion, including time-dependent mixing, are quantitatively assessed and compared for the first time in terms of mixing efficiency. Dead volume and uniformity index are assessed, and their suitability to produce practical results evaluated for the first time. In addition, a novel qualitative method is proposed to analyze the mixing conditions and the behaviour of a digester over time. A numerical tracer is defined as a scalar tracer obeying the non-diffusive advection-diffusion equation, different (logarithmic) intervals for concentration value defined, and the relative occupancy of each interval is evaluated. The results demonstrate that this method provides useful information on mixed and unmixed areas within the digester.

2. Materials and Methods

2.1. Assessment of Mixing

Mixing is assessed through the introduction of a numerical tracer. Numerically, the tracer's concentration is described through a scalar field obeying a non-diffusive advection-diffusion equation:

$$\partial_t \chi + (\mathbf{u} \cdot \nabla) \chi = 0 \ , \tag{1}$$

where χ is the tracer concentration, and $\mathbf{u}$ is the velocity vector field. At the initial timestep ($t = 0$), the tracer is seeded into different points of the digester. Numerically, this means that χ is initialized as $\chi = 1$ in small, localized portions of the computational domain, and as $\chi = 0$ elsewhere. The distribution of the scalar field $\chi(\mathbf{x})$ at the subsequent timesteps is used to assess mixing quality, as described in the following Sections.

2.1.1. Uniformity Index

The uniformity index (UI) is defined following Terashima et al. (2009). Let V_i be the volume of the i-th cell in the computational domain, and χ_i the (discretized) value of χ therein. The total volume of the computational domain V and the average tracer concentration $\overline{\chi}$ are:

$$V = \sum_i V_i \ , \tag{2}$$

$$\overline{\chi} = \frac{1}{V} \sum_i V_i \chi_i \ . \tag{3}$$

The uniformity index is defined as:

$$\mathrm{UI} := \frac{1}{2V\overline{\chi}} \sum_i |\chi_i - \overline{\chi}| \, V_i \ . \tag{4}$$

Following Terashima et al. (2009), it is straightforward to show that UI is bounded between

0 and 1, with $\chi = 0$ indicating perfect uniformity, and $\chi = 1$ total inhomogeneity, which means, numerically, the tracer being confined at the seeding locations only. For the case of perfect uniformity, $\chi_i = \overline{\chi}\ \forall i$, and hence:

$$\mathrm{UI}_{\mathrm{min}} = \frac{1}{2V\overline{\chi}} \sum_i \left|\overline{\chi} - \overline{\chi}\right| V_i = 0\ . \tag{5}$$

If the tracer is concentrated in a single cell s, we have $\chi_s = V/V_s\,\overline{\chi}$, and $\chi_{i \neq s} = 0$. Then:

$$\begin{aligned} \mathrm{UI}_{\mathrm{max}} &= \frac{\left|\frac{V}{V_s}\overline{\chi} - \overline{\chi}\right| V_s}{2V\overline{\chi}} + \frac{1}{2V\overline{\chi}} \sum_{i \neq s} \left|0 - \overline{\chi}\right| V_i \\ &= \frac{(V - V_s)\,\overline{\chi}}{2V\overline{\chi}} + \frac{(V - V_s)\,\overline{\chi}}{2V\overline{\chi}} = \frac{V - V_s}{V} \simeq 1 \qquad (V_s \ll V)\ . \end{aligned} \tag{6}$$

2.1.2. Dead Volume

The dead volume criterion was first introduced by Vesvikar and Al-Dahhan (2005). Contrary to the UI case, this method is based on fluid velocity rather than tracer concentration: at a given time, the maximum fluid velocity within the system is measured, and the portion of the computational domain where the velocity magnitude is below 5% of the maximum velocity is labelled as dead volume.

Dead volume is considered as cut off from the surrounding flow patterns; consequently, new influent sludge is considered unable to reach dead volume, and anaerobic digestion is considered as not taking place there. As such, a primary objective of mixing consists of minimizing dead volume.

2.1.3. Relative Occupancy of Concentration Intervals

The degree of uniformity of the tracer is assessed as follows. The interval of values $I \equiv [0,\,1]$ that χ can assume is decomposed into N sub-intervals $\{I_i\} \equiv I_1,\,\ldots,\,I_N$ such that $I_i \cup \cdots \cup I_N = I$. For each sub-interval I_i, the relative occupancy α_i is defined as:

$$\alpha_i := \frac{\int \mathrm{d}^3x \; \Xi_i(\chi(\mathbf{x}))}{\int \mathrm{d}^3x} \,, \qquad i = 1, \, \ldots, \, N \,, \tag{7}$$

where the rectangular functions $\Xi_i(\chi)$ are defined as:

$$\Xi_i(\chi) := \begin{cases} 1 \,, & \chi \in I_i \,; \\ 0 \,, & \chi \notin I_i \,; \end{cases} \qquad i = 1, \, \ldots, \, N \,. \tag{8}$$

This definition implies that $\sum_{i=1}^{N} \alpha_i = 1$. When the tracer field χ becomes uniform (and hence, the system is well-mixed), one single occupancy α_m becomes much larger than all the others, regardless of its particular value, but excluding α_1, where it was considered that $I_i \ni \chi \equiv 0$. In this latter case, in fact, the tracer has not been able to spread through the domain, with $\chi \simeq 1$ in the small seeding regions, and $\chi \simeq 0$ in the rest of the domain.

Given two different system configurations, described by the two sets of relative occupancies $\{\alpha_i\}$ and $\{\beta_i\}$ respectively, both with the same sub-domain decomposition $I_1, \, \ldots, \, I_N$, the first configuration is considered as better mixed if $\max_{i \neq 1} \alpha_i > \max_{j \neq 1} \beta_j$.

2.2. CFD Modelling

Below, the basic assumptions in modelling biogas-mixed sludge are described—a detailed description of the CFD model is reported elsewhere (Dapelo et al., 2015; Dapelo and Bridgeman, 2018).

2.2.1. Liquid Phase

Sludge is a complex mixture of water, flocculant and sedimenting matter, and biogas bubbles due to biogas mixing. Within this work, mixing was only considered from the perspective of providing a homogeneous environment for bacteria, with nutrients being spread evenly—the impact of mixing on sedimentation and flocculation prevention was ignored at this stage. This choice was justified by the fact that flocculation and sedimentation take place through time scales of days, if not years, whereas the simulations performed within this work spanned a physical time of 20 minutes. Consequently, the liquid and solid fractions were modelled together as a single continuous, constant-density liquid phase obeying the incompressible Navier-Stokes equations.

2.2.2. Rheology

Sludge is known to have a complex rheology (Eshtiaghi et al., 2013), that is a function of total solids content (TS), temperature (Achkari-Begdouri and Goodrich, 1992) and digestion progress (Hreiz et al., 2017). Non-Newtonian behaviour been shown to affect fluid flow patterns inside a digester (Wu and Chen, 2008) and consequently, non-Newtonian modelling has become an important element of CFD modelling of anaerobic digestion.

The most common and straightforward model is the pseudoplastic (Terashima et al., 2009; Wu, 2010, 2013; Bridgeman, 2012; Wu, 2014; Dapelo et al., 2015; Hurtado et al., 2015; Zhang et al., 2016; Sindall et al., 2017; Dapelo and Bridgeman, 2018; Lebranchu et al., 2017; Meister et al., 2018) in which apparent viscosity μ and shear rate magnitude $|\dot{\gamma}|$ obey a power-law relationship:

$$\mu = K\,|\dot{\gamma}|^{n-1}\ , \tag{9}$$

where “pseudoplastic” means $n < 1$, and K is the consistency coefficient.

A more recent approach consists of using the Herschel-Bulkley model (Craig et al., 2013; Hurtado et al., 2015; Dapelo and Bridgeman, 2018). Here, the power-law flow occurs only if the shear stress exceeds a critical value τ_0:

$$\mu = \tau_0\,|\dot{\gamma}|^{-1} + K\,|\dot{\gamma}|^{n-1}\ . \tag{10}$$

In the work reported here, both the power-law (Eq. 9) and the Herschel-Bulkley model

(Eq. 10) were adopted, together with a Newtonian model for comparison. For the power-law model, data from Landry et al. (2004) was adopted for TS value of 2.5, 5.4 and 7.5%, while for the Herschel-Bulkley, data was taken from Baudez et al. (2013) for a TS value of 1.85%. These values were chosen in order to cover the range of the most common feeds for industrial digesters, and for comparison with previous work (Wu, 2010, 2012a; Bridgeman, 2012) and with previous validation and application of the CFD model used in this work (Dapelo et al., 2015; Dapelo and Bridgeman, 2018) and dependence on digestion progress was ignored because of the semi-continuous nature of the considered digesters. Table 1 reports the rheological models used in this work in numerical detail.

[Table 1 about here.]

As in Dapelo and Bridgeman (2018), the numerical solvers switched to a Newtonian model continuously when the local shear rate dropped below the user-defined threshold of 0.001 s^{-1} in order to avoid a singularity at $|\dot{\gamma}| = 0$. When appropriate, the relations described in Eq. 9 and 10 with the coefficients reported in Table 1 were extrapolated beyond the experimentally-measured range. Mesophilic anaerobic digestion maintains constant temperature conditions (35 $^\circ\mathrm{C}$), and therefore sludge rheology's dependence on temperature (Baudez et al., 2013) was ignored. As discussed in Dapelo et al. (2015), the values of density for the TS range considered vary from 1,000.36 to 1,001.73 $\mathrm{kg\,m^{-3}}$ (Achkari-Begdouri and Goodrich, 1992), which differ for less than 1% from water density at 35 degrees (994 $\mathrm{kg\,m^{-3}}$), and therefore density was approximated to 1,000 $\mathrm{kg\,m^{-3}}$ in all cases.

2.2.3. Bubble Phase & Multiphase Model

Mixing in biogas-mixed anaerobic digesters is driven by the rise of bubble plumes. This means that the faithful simulation of flow patterns throughout the computational domain requires robust modelling of the bubble-liquid phase momentum exchange, but the details of liquid phase motion around the bubbles are unimportant. A solution was proposed and validated by Dapelo et al. (2015) and applied for the first time to full-scale design by Dapelo and Bridgeman (2018), and consisted of an Euler-Lagrangian multiphase CFD model, which was shown in the literature to be an effective balance between robustness, economy, flexibility and accuracy given the requirements described above. As described in Sections 2.2.1 and 2.2.2, the water-TS mixture was considered as a single, non-Newtonian liquid phase, while the gas phase was modelled as a bubble ensemble subjected to the following assumptions: (*i*) one bubble per parcel, (*ii*) spherical bubbles, and (*iii*) pointwise bubbles.

The inter-phase momentum exchange was modelled as a two-way coupling (liquid phase and single bubbles exchange momentum each other, but bubbles do not between themselves), this being justified by the observation in Dapelo et al. (2015); Dapelo and Bridgeman (2018) and in the simulations performed within this work, that the bubbles are always well-distanced from one another. Following Dapelo et al. (2015), the force acting on a bubble from the surrounding liquid phase (and, consequently, the same force with opposite sign, acting on the surrounding liquid phase from the bubble) consisted of the sum of buoyancy, drag as in Dewsbury et al. (1999) and lift as in Tomiyama et al. (2002). In order to compute the drag term correctly, the particle Reynolds number was determined locally, from the sum of liquid phase apparent and eddy viscosity.

Nominal bubble size is a required input data to compute inter-phase force, but no data are available in the literature on bubble diameter within anaerobic digesters. Dapelo and Bridgeman (2018) performed CFD simulations with three different bubble sizes (2, 6 and 10 cm diameter), and showed that velocity and viscosity flow patterns were only marginally affected by the choice of the bubble size. Consequently, for this work, only the maximum bubble size considered in Dapelo and Bridgeman (2018) of d = 10 cm was chosen in order to minimize the computational expense.

2.2.4. *Meshing*

A cylindrical digester with an inclined base was simulated (Fig. 1).

[Figure 1 about here.]

In the first instance, a series of twelve nozzles, equally-spaced along a circle at the sloped bottom of the tank was considered. A second series, with the nozzles placed along a concentric circle of different diameter, was subsequently considered in an amended design alongside the original one. The geometric details are reported in Table 2.

[Table 2 about here.]

The mesh consisted of a $\pi/6$ radian wedge, with a single nozzle per nozzle series lying on the symmetry plane of the wedge. Four grids were generated (Table 3).

[Table 3 about here.]

The computational work was undertaken using the BlueBEAR high performance computing facility at the University of Birmingham. Each simulation was run in parallel on 12-core Intel Xeon E5-2690 v3 Haswell sockets running at 2.6GHz with 128 GB RAM, for a total of 36 cores. OpenFOAM 2.3.0 with user-modified solver and libraries for the biogas phase, was used to run the computational work. The computational runtime was between ten hours and five days.

The turbulent motion of the liquid around the bubbles was modelled through the Reynolds stress Launder-Gibson model (Gibson and Launder, 1978; Dapelo et al., 2015; Dapelo and Bridgeman, 2018).

The timestep was defined dynamically as in Dapelo et al. (2015); Dapelo and Bridgeman (2018), via computation of the maximum Courant number. For a given cell, i, of linear magnitude L_i where the fluid velocity is $|\mathbf{u}_i|$, given the timestep Δt, the Courant number is defined as:

$$\mathrm{Co}_i = \frac{|\mathbf{u}_i|\ \Delta t}{L_i}\ . \tag{11}$$

The maximum Courant number, Co, is the maximum value of Co_i over i. Following Dapelo et al. (2015); Dapelo and Bridgeman (2018), after a small initial value of 10^{-5} s, the timestep was corrected at each iteration in order to keep the maximum Courant number near, but less than, the limit of 0.2. Following this procedure, after the initial transient, the timestep was observed to be between 0.0013 and 0.14 seconds.

At each timestep, the solution was considered as converged when the residual for the pressure fell below 10^{-7}, and for all the other quantities below 10^{-6}.

The initial condition consisted of a system configuration with a fully-developed bubble plume. In order to obtain this system configuration, a series of preliminary, first-order transient PISO runs was performed for a computational time of 60 s. In these preliminary runs, the bubble plume developed from a state with no bubble and no liquid phase motion. Different initial conditions for χ ("seeding") were defined as follows: χ = 0 everywhere, apart from small, selected portions of the domain, where χ = 1. A more detailed discussion on the specific seeding choices is reported below, in Section 3. The last timestep of the preliminary runs served as the initial condition for a series of main, second-order transient PISO runs, which was performed for an additional 1,140 s and for an overall computational time of 1,200 s in order to replicate the mixing time reported in Table 2. As in Dapelo and Bridgeman (2018), binary files were collected for every integer-second timestep.

The boundary conditions follow Dapelo and Bridgeman (2018) and are described as follows. Top: zero constant value for pressure, free-slip for all the other fields. Wall/bottom: constant zero for velocity, zero gradient for tracer concentration, standard wall function for turbulent dissipation and Reynolds stess, and pressure adjusted such that the velocity flux is zero.

Front/back: cyclic for all the fields. The values of C_μ, κ and E for the wall functions were set to 0.09, 0.41 and 9.8 respectively. The initial conditions for the preliminary runs were: 4.95 $10^{-4}\,\mathrm{m}^2\,\mathrm{s}^{-3}$ for the ε field, zero for p, u and R_{ij}. The differencing schemes used were: linear for interpolations, limited central differencing for the Gradient operator, linear for the Laplacian, Van Leer for all the other spatial operators, first-order Eulerian scheme for the time derivative in the preliminary runs and second-order backward for the main runs.

3. Results and Discussion

Four series of runs were performed under the following conditions: (i) biogas injection through the original nozzle series at the distance R_1 from the axis (labelled as "Original"); (ii) injection through the additional series at distance R_2 ("New"); (iii) switching biogas injection from the original to the new nozzle series every minute and vice-versa, starting from injecting from the original ("1 min switch"); and (iv) switching every five minutes ("5 min switch").

The series of runs were repeated for all the rheologies reported in Table 1, and for two different seedings, as shown in Figure 2. The small triangles on the inclined bottom represent the location of the nozzle series.

[Figure 2 about here.]

In the seeding configuration labelled as "Seed 1", the seeding was performed in a restricted area near the sludge feed location in the digester, while in "Seed 2", the seeding was performed uniformly throughout the domain. This scenario was considered in order to investigate both how new sludge is spread throughout the digester ("Seed 1"), and how further mixing of pre-existing sludge occurs ("Seed 2").

In Dapelo and Bridgeman (2018), it was concluded that the value of input mixing power of the original design was excessive, and could be halved without compromising mixing quality. Hence, the value of biogas flow rate, $Q = Q_{\max}/2$ = 2.3585 $10^{-3}\,\mathrm{m}^3\mathrm{s}^{-1}$ was used in all the computational work reported here.

3.1. Mesh Independence

Two grid independence tests were performed following Celik et al. (2008). The values of uniformity index and relative dead volume were computed at t = 300 s for each of the grids considered in this work. The results of the tests are reported in Table 4.

[Table 4 about here.]

In all the cases apart from the relative dead volume in the Newtonian case, Grids 1, 2 and 3 fell well within the asymptotic range of convergence, while Grid 4 was found to be outside. Dapelo and Bridgeman (2018) performed a similar test on average shear rate and found that Grid 1 was outside the asymptotic range of convergence. This was attributed to the fact that bubble size was no longer negligible on the finest grid. In light of these findings and considering the need to reduce computational expense where possible, Grid 2 was chosen for the numerical work reported here.

3.2. Evaluation of Uniformity Index

Fig. 3 shows the value of the uniformity index over time. The quantities $t_{0.10}$ and $t_{0.05}$ are the times the system takes for the uniformity index to fall below 0.1 and 0.05 respectively, and can be interpreted as the times the system needs to reach a degree of mixing of 90% and 95% respectively.

[Figure 3 about here.]

The values of $t_{0.10}$ and $t_{0.05}$ are reported in Table 5.

[Table 5 about here.]

In the “Original” configuration, new sludge (“Seed 1”) remained close to the injection zone, with the exception of a modest displacement in the 2.5% TS case towards the end of the simulation run. Pre-existing sludge (“Seed 2”) was spread throughout the domain, with an acceleration occurring once again in the 2.5% TS case at around the end of the run. Crucially, however, the uniformity index never fell below 0.1 in both cases, thus indicating ineffective mixing.

In the “New” configuration, a marginal improvement of the mixing conditions for new sludge was observed, when compared to the “Original”, while no significant change occurred for old sludge (“Seed 2”). However, as in the “Original” configuration, the uniformity factor did not fall below 0.1.

In the “1 min switch” configuration, a significant improvement of the mixing conditions was observed. The uniformity index dropped after around 120 s for “Seed 1” (around 60 s for “Seed 2”) and, with the exception of the Newtonian case, fell below 0.1 after 580—680 s (380—510 s), and below 0.05 after 720—870 s (510—680 s). This showed that: (*i*) the strategy of switching biogas injection between two nozzle series every minute was effective in improving mixing; and (*ii*) this strategy achieved a satisfactory level of mixing (i.e., UI $<$ 0.1 for “Seed 1”) after approximately 600 s, which corresponded to half of the original design’s mixing time, and hence, half of the overall mixing energy determined in Dapelo and Bridgeman (2018), and one quarter of the original design’s overall mixing energy.

The “5 min switch” configuration displayed a trend similar to the “1 min switch”. However, the reduction in the uniformity factor took place at a slower rate: $t_{0.10}$ occurred 140—190 s later than in “1 min switch” for “Seed 1” (130—180 s for “Seed 2”), while $t_{0.05}$ was delayed by 100—170 s (100—310 s). This indicated that, despite constituting an improvement if compared to “Original” and “New” configurations, “5 min switch” was less effective than “1 min switch”.

3.3. Evaluation of Dead Volume

The value of the relative dead volume over time is shown in Figure 4. This value displayed significant variability, thus making it impossible to derive any evaluation of the degree of mixing from it.

[Figure 4 about here.]

This behaviour may be an artefact of the way in which dead volume is defined. As discussed in Section 2.1.2, the definition of dead volume depends on the value of the maximum velocity. This makes the value of dead volume a function of the fluctuation of the maximum velocity. However, Fig. 4 shows strong fluctuations of the maximum velocity in all the simulations, throughout the whole simulated time interval, and hence, giving rise to the strong variability of the dead volume.

This result shows that, despite being frequently used in the previous literature, relative dead volume is an inappropriate criterion to assess mixing.

3.4. Evaluation of Relative Occupancy Intervals

The evolution of the relative occupancy intervals is displayed in Fig. 5.

[Figure 5 about here.]

Ten intervals, following a logarithmic scale, were chosen, as shown in the figures' legends. In this way, it was possible to investigate the relative importance of different orders of magnitude for the value of χ—in particular, of very low concentration $\chi < 10^{-9}$.

In the "Original" configuration, "Seed 1", the relative occupancy of very low concentrations α_0 remained dominant for almost the entire duration of the runs, with a marginal drop occurring only at the end of the simulated time interval. This indicated that the mixing mechanism was unable to spread effectively new sludge away from the injection zone.

In the "Seed 2" case, α_0 was shown to drop at the very start of the mixing time, thus indicating that old sludge actually undertook mixing. However, coexistence of all the intervals and failure of α_0 to vanish showed that mixing occurred only partially.

In the "New", both "Seed 1" and "Seed 2" cases show a behaviour qualitatively similar to the “Original, Seed 2” case. This means that new sludge is spread throughout the digester and old sludge undertakes mixing, but both only to a partial extent.

In the “1 min switch” and “5 min switch” configurations, α_0 dropped rapidly and vanished after a time around the corresponding $t_{0.10}$. At the same time, a single interval, different from I_0, became dominant. This means that mixing could be considered as complete after this time.

Finally, the evaluation of the relative occupancy intervals showed that the behaviour of the Newtonian model differed qualitatively from the non-Newtonian. This was evident from both observing the quantitative values of the uniformity index, and the qualitative behaviour of the relative occupancy intervals, in the “Original” and “New” configurations. Thus, the choice of Newtonian in place of non-Newtonian rheology altered the flow patterns, as previously noted by Wu and Chen (2008). For this reason, despite the fact that several researchers have adopted Newtonian rheology to model sludge in previous work (Vesvikar and Al-Dahhan, 2005; Karim et al., 2007; Meroney and Colorado, 2009), results shown here indicate that is approach should be avoided.

4. Conclusions

The use of uniformity index is encouraged over dead volume as a quantitative mixing evaluation criterion.

Switching nozzle series every minute greatly improved mixing quality for all the rheology models, with the optimum degree of mixing being reached after 600 s from the onset of mixing.

Qualitative observations showed that the Newtonian system behaves differently from all the non-Newtonian models. Accordingly, the use of Newtonian models is discouraged.

Supplementary Material

E-supplementary data, showing more graphical details of the mesh used in this work, can be found in online version of the paper.

Acknowledgments

The details of the digester geometry were kindly provided by Peter Vale, Severn Trent Water Ltd., whom the authors gratefully acknowledge.

The computational work reported in this paper was undertaken using the BlueBEAR high performance computing facility at the University of Birmingham, UK. The authors are grateful for the facility and support provided.

The first author was funded via a University of Birmingham Postgraduate Teaching Assistantship award, and then via a University of Bradford Postdoctoral research assistant contract, who provided financial support.

Declarations of interest:

None.

References

1. Achkari-Begdouri, A., Goodrich, P.R., 1992. Rheological properties of Moroccan dairy cattle manure. Bioresource Technology 40, 225–233.

2. Baudez, J.C., Slatter, P., Eshtiaghi, N., 2013. The impact of temperature on the rheological behaviour of anaerobic digested sludge. Chemical Engineering Journal 215-216, 182–187.

3. Brade, C.E., Noone, G.P., 1981. Anaerobic sludge digestion: Need it be expensive? Making more of existing resources. Water Pollution Control 80, 70–94.

4. Bridgeman, J., 2012. Computational fluid dynamics modelling of sewage sludge mixing in an anaerobic digester. Advances in Engineering Software 44, 54–62.

5. Camp, T.R., Stein, P.C., 1943. Velocity gradients and internal work in fluid motion. Journal of the Boston Society of Civil Engineering 85, 218–237.

6. Celik, I.B., Ghia, U., Roache, P.J., Freitas, C.J., Coleman, H., Raad, P.E., 2008. Procedure for Estimation and Reporting of Uncertainty Due to Discretization in CFD Applications. Journal of Fluids Engineering 130, 078001.

7. Clark, M.M., 1985. Critique of Camp and Stein's RMS Velocity Gradient. Journal of Environmental Engineering 111, 741–754.

8. Craig, K.J., Nieuwoudt, M.N., Niemand, L.J., 2013. CFD simulation of anaerobic digester with variable sewage sludge rheology. Water Research 47, 4485–4497.

9. Dapelo, D., Alberini, F., Bridgeman, J., 2015. Euler-Lagrange CFD modelling of unconfined gas mixing in anaerobic digestion. Water Research 85, 497–511.

10. Dapelo, D., Bridgeman, J., 2018. Euler-Lagrange Computational Fluid Dynamics simulation of a full-scale unconfined anaerobic digester for wastewater sludge treatment. Advances in Engineering Software 117, 153–169.

11. Dewsbury, K., Karamanev, D., Margaritis, a., 1999. Hydrodynamic characteristics of free rise of light solid particles and gas bubbles in non-Newtonian liquids. Chemical Engineering Science 54, 4825–4830.

12. Eshtiaghi, N., Markis, F., Yap, S.D., Baudez, J.C., Slatter, P., 2013. Rheological characterisation of municipal sludge: A review. Water Research 47, 5493–5510.

13. European Environment Agency, 2015. Waterbase - UWWTD: Urban Waste Water Treatment Directive reported data. Technical Report. URL: http://www.eea.europa.eu/data-and-maps/data/waterbase-uwwtd-urban-waste-water-treatment-directive-4.

14. Gibson, M.M., Launder, B.E., 1978. Ground effects on pressure fluctuations in the atmospheric boundary layer. Journal of Fluid Mechanics 86, 491–511.

15. Hreiz, R., Adouani, N., Fünfschilling, D., Marchal, P., Pons, M.N., 2017. Rheological characterization of raw and anaerobically digested cow slurry. Chemical Engineering Research and Design 119, 47–57.

16. Hurtado, F., Kaiser, A., Zamora, B., 2015. Fluid dynamic analysis of a continuous stirred tank reactor for technical optimization of wastewater digestion. Water Research 71, 282–293.

17. Karim, K., Thoma, G.J., Al-Dahhan, M.H., 2007. Gas-lift digester configuration effects on mixing effectiveness. Water Research 41, 3051–3060.

18. Kress, P., Nägele, H.J., Oechsner, H., Ruile, S., 2018. Effect of agitation time on nutrient distribution in full-scale CSTR biogas digesters. Bioresource Technology 247, 1–6.

19. Landry, H., Laguë, C., Roberge, M., 2004. Physical and rheological properties of manure products. Applied Engineering in Agriculture 20, 277–288.

20. Lebranchu, A., Delaunay, S., Marchal, P., Blanchard, F., Pacaud, S., Fick, M., Olmos, E., 2017. Impact of shear stress and impeller design on the production of biogas in anaerobic digesters. Bioresource Technology 245, 1139–1147.

21. Meister, M., Rezavand, M., Ebner, C., Pümpel, T., Rauch, W., 2018. Mixing non-Newtonian flows in anaerobic digesters by impellers and pumped recirculation. Advances in Engineering Software 115, 194–203.

22. Meroney, R.N., Colorado, P.E., 2009. CFD simulation of mechanical draft tube mixing in anaerobic digester tanks. Water Research 43, 1040–1050.

23. Owen, W.F., 1982. Anaerobic Treatment Processes, in: Energy in wastewater tall wreatment. Prentice-Hall, Inc., Englewood Cliffs, NJ.

24. Sindall, R.C., Bridgeman, J., Carliell-Marquet, C., 2013. Velocity gradient as a tool to characterise the link between mixing and biogas production in anaerobic waste digesters. Water Science and Technology 67, 2800–2806.

25. Sindall, R.C., Dapelo, D., Leadbeater, T., Bridgeman, J., 2017. Positron emission particle tracking (PEPT): A novel approach to flow visualisation in lab-scale anaerobic digesters. Flow Measurement and Instrumentation 54, 250–264.

26. Tchobanoglous, G., Burton, Franklin, L., Stensel, H.D., 2010. Wastewater Engineering. Metcalf & Eddy, Inc.

27. Terashima, M., Goel, R., Komatsu, K., Yasui, H., Takahashi, H., Li, Y.Y., Noike, T., 2009. CFD simulation of mixing in anaerobic digesters. Bioresource Technology 100, 2228–2233.

28. Tomiyama, A., Tamai, H., Zun, I., Hosokawa, S., 2002. Transverse migration of single bubbles in simple shear flows. Chemical Engineering Science 57, 1849–1858.

29. Vesvikar, M.S., Al-Dahhan, M.H., 2005. Flow pattern visualization in a mimic anaerobic digester using CFD. Biotechnology and Bioengineering 89, 719–732.

30. WaterUK, 2012. Sustainability Indicators 2010-2011. Technical Report. Water UK. London. URL: http://water.wuk1.emsystem.co.uk/home/news/press-releases/indicators2010-11/water-uk---sustainability-report-2010-11.pdf{%}5Cnfiles/1080/WaterUK{_}2012{_}SustainabilityIndicators2010-2011.pdf.

31. Wu, B., 2010. CFD simulation of gas and non-Newtonian fluid two-phase flow in anaerobic digesters. Water Research 44, 3861–3874.

32. Wu, B., 2012a. CFD simulation of mixing for high-solids anaerobic digestion. Biotechnology and Bioengineering 109, 2116–2126.

33. Wu, B., 2012b. Integration of mixing, heat transfer, and biochemical reaction kinetics in anaerobic methane fermentation. Biotechnology and Bioengineering 109, 2864–2874.

34. Wu, B., 2013. Advances in the use of CFD to characterize, design and optimize bioenergy systems. Computers and Electronics in Agriculture 93, 195–208.

35. Wu, B., 2014. CFD simulation of gas mixing in anaerobic digesters. Computers and Electronics in Agriculture 109, 278–286.

36. Wu, B., Chen, S., 2008. CFD simulation of non-Newtonian fluid flow in anaerobic digesters. Biotechnology and Bioengineering 99, 700–711.

37. WWAP (World Water Assessment Programme), 2012. The United Nations World Water Development Report 4: Managing Water under Uncertainty and Risk. Technical Report. UNESCO. Paris. URL: http://www.unesco.org/new/fileadmin/MULTIMEDIA/HQ/SC/pdf/WWDR4Volume1-ManagingWaterunderUncertaintyandRisk.pdf.

38. Zhang, Y., Yu, G., Yu, L., Siddhu, M.A.H., Gao, M., Abdeltawab, A.A., Al-Deyab, S.S., Chen, X., 2016. Computational fluid dynamics study on mixing mode and power consumption in anaerobic mono- and co-digestion. Bioresource Technology 203, 166–172.

List of Tables

List of Figures

Table 1: Rheological properties of sludge, from Dapelo and Bridgeman (2018). "$|\dot{\gamma}|$ range" refers to the limits of the shear range interval in which the experimental measurements were performed.

	TS (%)	τ_0 (Pa)	K ($\mathrm{Pa\,s}^n$)	n (–)	$\lvert\dot{\gamma}\rvert$ range (s^{-1})
Power-law Landry et al. (2004)	2.5	0	0.042	0.710	226–702
	5.4	0	0.192	0.562	50—702
	7.5	0	0.525	0.533	11—399
Herschel-Bulkley Baudez et al. (2013)	1.85	0.092	0.169	0.308	0.01–30
Newtonian	–	0	12	1	–

Table 2: Details of the digester geometry, from Dapelo and Bridgeman (2018). Sludge feed inlet is located on a side wall, at a height $h/4$ below the top sludge level. Courtesy of Severn Trent Water Ltd.

External diameter	D_{ext}	14.63 m
Diameter at the bottom of the frustum	D_{int}	1.09 m
Cylinder height	h	14 m
Frustum height	h_0	3.94 m
Distance of original nozzle series from axis	R_1	1.83 m
Distance of new nozzle series from axis	R_2	5.49 m
Distance of nozzles from bottom	h_{noz}	0.3 m
Gas flow rate per nozzle	$Q_{\max}$	4.717 10^{-3} $\mathrm{m^3s^{-1}}$
Mixing time		20 min in an hour

Table 3: Details of the grids. From Dapelo and Bridgeman (2018).

Id.	Number of cells	Max skewness	Max aspect ratio	Non-ortho max	Non-ortho avg	Volume min (m^3)	Volume max (m^3)	Vol wedge (m^3)
1	394,400	1.123	13.24	30.03	14.00	1.500e-5	1.011e-3	215.8
2	98,420	1.064	9.974	30.00	13.66	3.158e-5	4.241e-3	215.8
3	36,720	1.112	10.53	30.03	13.78	3.333e-5	1.116e-2	215.3
4	18,760	1.304	13.54	30.01	13.84	4.286e-5	2.144e-2	215.3

Table 4: GCI analysis

	Uniformity Index					Relative dead volume				
	2.5 TS	5.4 TS	7.5 TS	He.Bu.	Newton	2.5 TS	5.4 TS	7.5 TS	He.Bu.	Newton
Grid 4	0.132	0.13	0.256	0.235	0.294	0.78	0.65	0.5893	0.7399	0.23
Grid 3	0.194	0.20	0.248	0.239	0.347	0.72	0.58	0.5834	0.7421	0.24
Grid 2	0.3447	0.350	0.440	0.440	0.571	0.962	0.938	0.8909	0.9024	0.25
Grid 1	0.347823	0.383	0.4340	0.445438	0.5954	0.94466	0.952361	0.90147	0.967	0.30
p_2	5.479	5.201	17.88	22.03	8.534	7.375	8.709	22.26	24.13	1.920
p_1	16.06	6.986	14.31	14.64	9.628	10.64	13.20	13.99	4.797	0.959
$\mathrm{GCI2}_{43}$	0.091	0.10	1.6e-4	2.3e-5	0.015	0.012	0.011	1.3e-5	2.1e-6	0.073
$\mathrm{GCI2}_{32}$	0.20	0.21	0.0071	0.0027	0.070	0.063	0.064	0.0019	6.3e-4	0.11
$\mathrm{GCI1}_{32}$	0.011	0.12	0.017	0.017	0.052	0.026	0.020	0.014	0.10	0.25
$\mathrm{GCI1}_{21}$	6.6e-6	0.0043	2.2e-5	1.87e-5	5.8e-4	1.6e-4	4.4e-5	2.3e-5	0.011	0.34
Asymp.2	0.123	0.140	2.89e-4	4.04e-5	0.026	0.032	0.021	2.98e-5	9.63e-6	0.415
Asymp.1	1.006	1.092	1.046	1.013	1.041	1.125	1.015	1.013	1.072	0.484

Table 5: Time (in s) to obtain UI < 0.1 and UI < 0.05.

	Original series		New series		1 min switch		5 min switch	
$t_{0.10}$	Sd. 1	Sd. 2	Sd. 1	Sd. 2	Sd. 1	Sd. 2	Sd. 1	Sd. 2
2.5 TS	—	—	—	—	580	380	790	620
5.4 TS	—	—	—	—	580	410	930	700
7.5 TS	—	—	—	—	680	550	1,020	950
Herschel-Bulkley	—	—	—	—	680	510	910	730
Newtonian	—	—	—	—	1,030	780	1,090	980
$t_{0.05}$	Sd. 1	Sd. 2	Sd. 1	Sd. 2	Sd. 1	Sd. 2	Sd. 1	Sd. 2
2.5 TS	—	—	—	—	720	510	890	720
5.4 TS	—	—	—	—	740	550	1,100	910
7.5 TS	—	—	—	—	850	730	1,180	1,150
Herschel-Bulkley	—	—	—	—	870	680	1,090	1,040
Newtonian	—	—	—	—	—	1,080	—	1,120

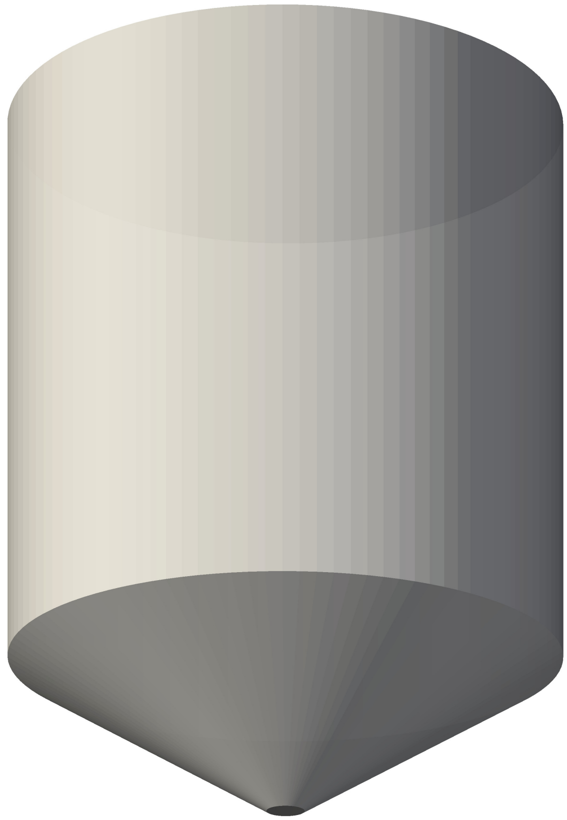

Figure 1: Computational domain. Illustrative view, from Dapelo and Bridgeman (2018).

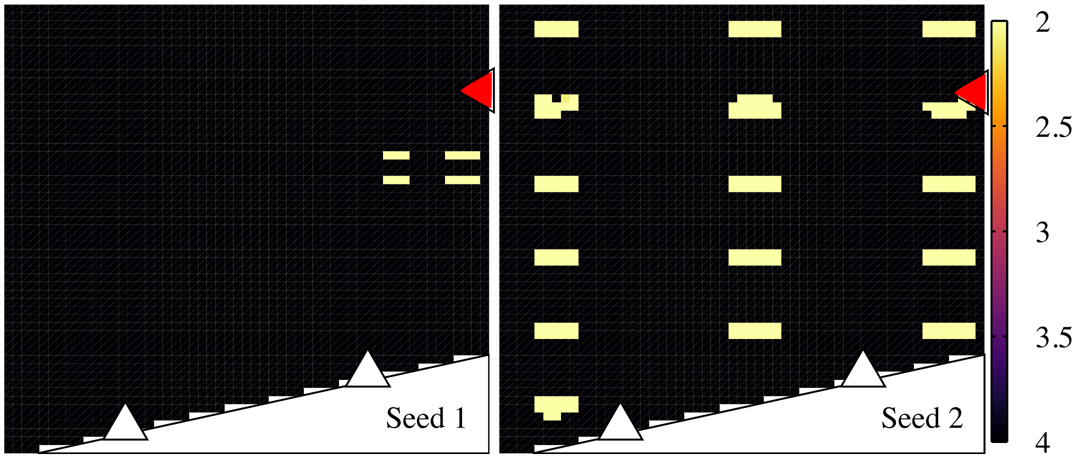

Figure 2: Seeding. Tracer concentration, logarithmic scale. The white triangles indicate where biogas injection occurred; the red triangles indicate sludge feed location.

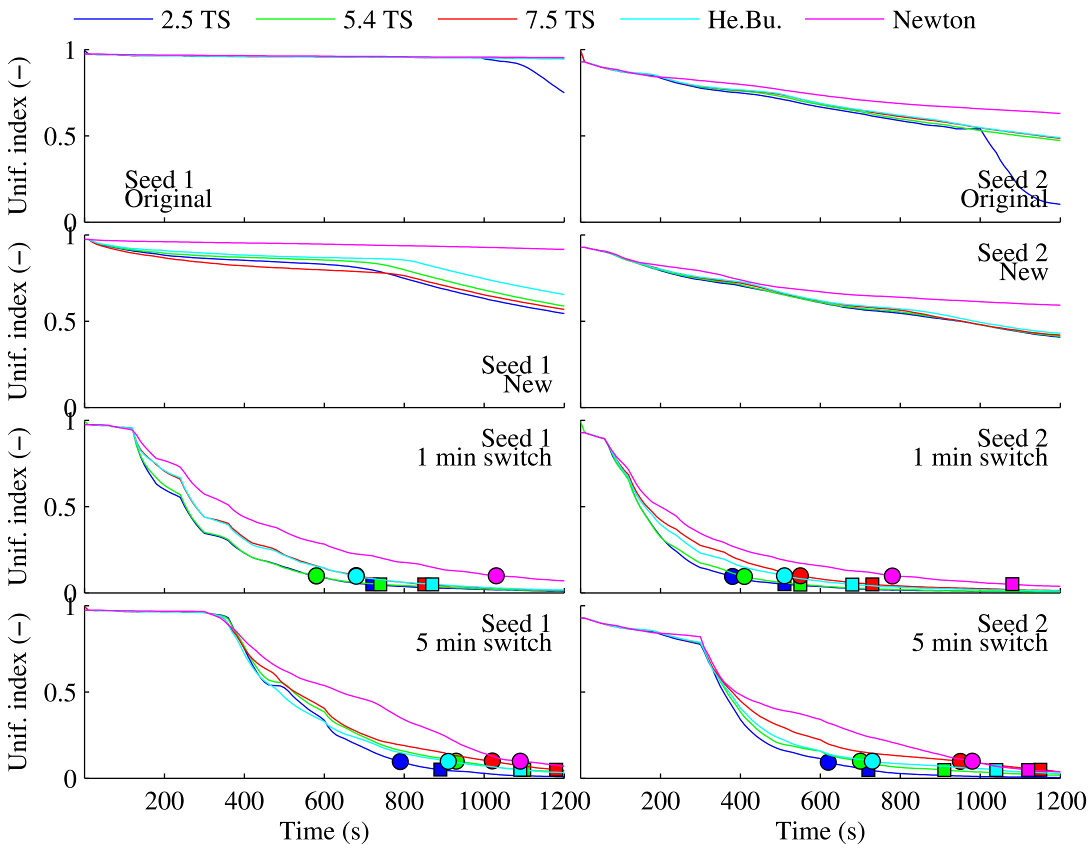

Figure 3: Uniformity index. Uniformity index over time for all the rheological models. $t_{0.10}$ and $t_{0.05}$ are marked with a circle and a square respectively.

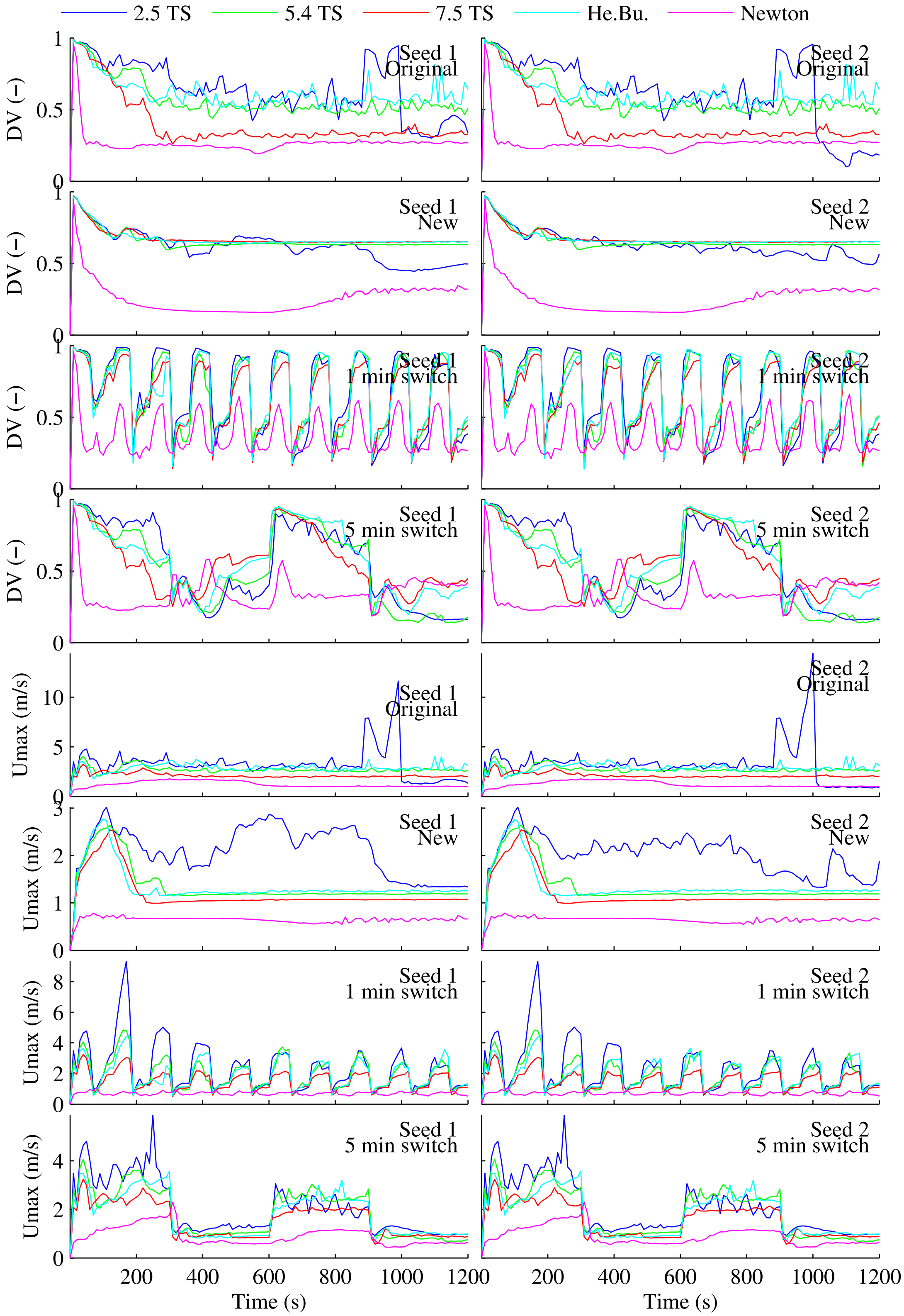

Figure 4: Dead volume. Relative dead volume and maximum velocity over time for all the rheological models.

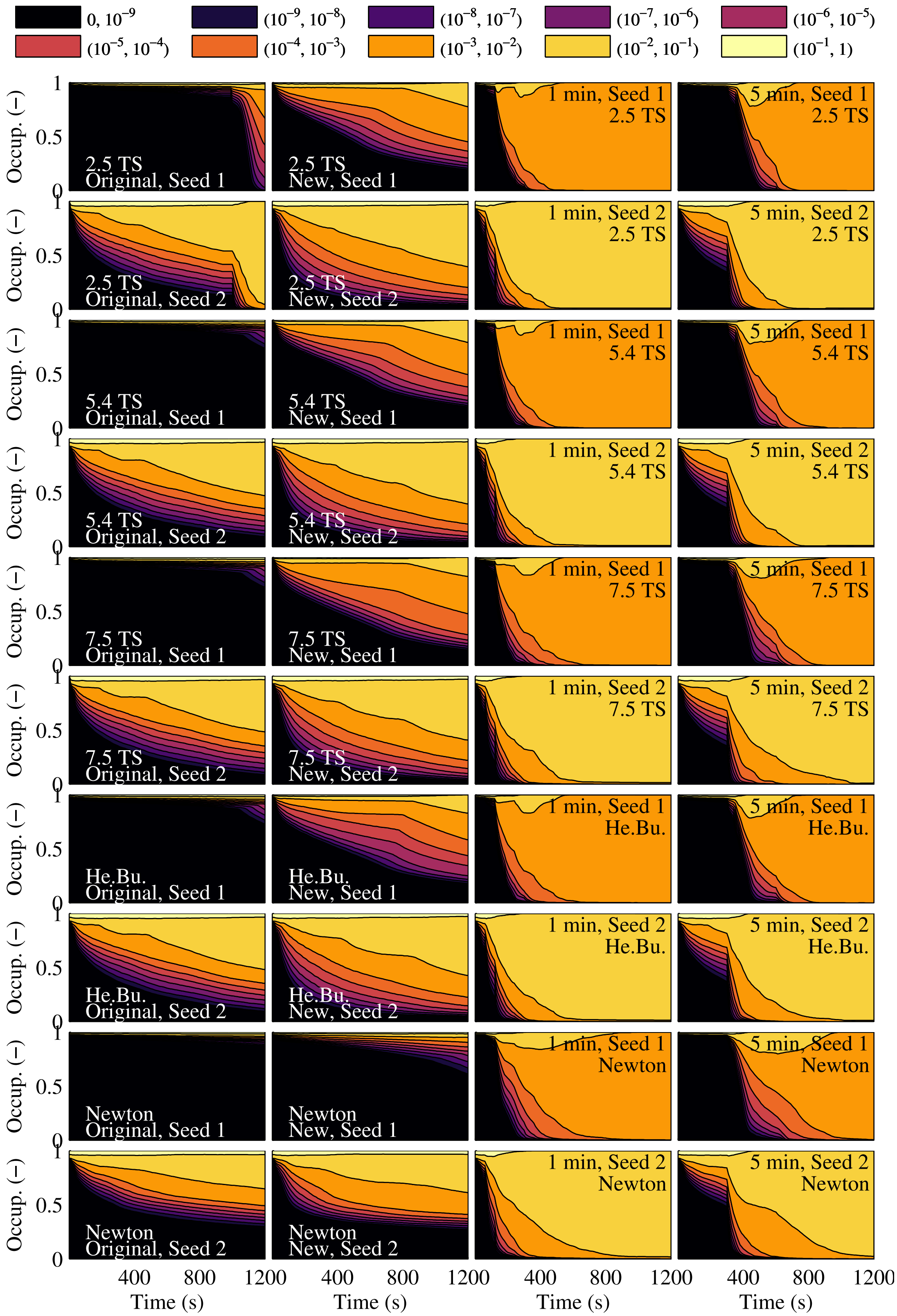

Figure 5: Relative occupancy. Relative occupancy intervals over time for all the rheological models.